AD-A172 828 PHYSICAL CONCEPTS AND MODELING PROCEDURES FOR PICOSECOND AND SUBPICOSECON..(U) STANFORD UNIV CA EDWARD L GINZTON LAB OF PHYSICS B A AULD ET AL. AUG 86 1/1

UNCLASSIFIED N00014-85-K-0301 F/G 9/3 NL

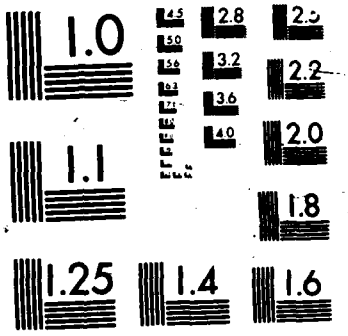
1.0
1.1
1.25
1.4
1.6
1.8
2.0
2.2
2.8
3.2
3.6
4.0

Edward L. Ginzton Laboratory
W. W. Hansen Laboratories of Physics
Stanford University
Stanford, California 94305-4028

Interim Report
to
Office of Naval Research
of
A Program of Research
on
Physical Concepts and Modeling Procedures for Picosecond and Subpicosecond Distributed Circuits

Contract N00014-85-K-0381

Principal Investigators
B. A. Auld
D. M. Bloom

August 1986

PHYSICAL CONCEPTS AND MODELING PROCEDURES FOR PICOSECOND AND SUBPICOSECOND DISTRIBUTED CIRCUITS

Overview

Research work under this contract has been focused on three primary projects: modeling and development of a nonlinear transmission line for the production of picosecond pulses; modeling and development of a tapered microstrip coupler; and the modeling and characterization of the accuracy of the electrooptic sampling system. The projects share the goal of facilitating the development of ultrafast electronics and the ability to characterize them.

Nonlinear Transmission Line for Electrical Pulse Compression

Very wide bandwidth electronic instrumentation is needed for the testing and characterization of millimeter-wave analog and picosecond-delay digital GaAs integrated circuits. While frequency-domain instruments (vector network analysers) are available for waveguide bands as high in frequency as 60-90 GHz, these instruments are inconvenient for the testing of pulsed systems and for time-domain reflectometry of broadband waveguiding systems. Currently available time-domain instruments include sampling oscilloscopes and optical systems using pulsed lasers in conjunction with photoconductors or optical nonlinearities. Sampling oscilloscopes have limited bandwidth (risetimes of c.a. 25 ps.), while the optical systems are costly and complex. All-electronic picosecond pulse sources and detectors are critical components for the development of picosecond resolution time-domain instrumentation. Picosecond pulse sources would also find applications in very high-speed digital switches and multiplexers (in conjunction with diode bridges serving as the switching element), and in fast analog systems. Picosecond electrical pulses will prove useful in the investigation of semiconductor transport properties occurring on the picosecond time scale.

On this contract, we had proposed to investigate a nonlinear transmission medium whose function is the compression of electrical wavefronts to picosecond duration. The proposed structure is a GaAs integrated circuit on which a relatively high-impedance transmission line is periodically loaded with reverse-biased Schottky diodes serving as nonlinear, voltage-dependent capacitors. The wave propagation speed, given by $s(V) = 1/\sqrt{lc(V)}$, where l is the line inductance per unit length, and $c(V)$ is the sum of the Schottky (nonlinear, voltage-dependent) and line capacitances per unit length, is function of voltage; given $c(V)$ decreasing with voltage, a positive-going step function of finite risetime input to the line will emerge with its risetime reduced. The risetime of the final compressed transient is limited to some finite, nonzero, value by several sources of dispersion arising within the structure; at the time of the proposal we had identified the fundamental limitation as the diode *RC* cutoff frequency and had projected on this basis that risetimes of 0.6 ps should be attainable. We proposed to further investigate the limitations on compressed risetime and to fabricate both initial (scale) models and fully

integrated monolithic compressors.

In addition to the diode's *RC* cutoff frequency, several other sources of dispersion contribute significantly to the limitations on the final compressed electrical risetime. In the compressor, the nonlinear elements are connected at finite spacings along a transmission line; the resulting periodic structure has an associated cutoff frequency. The effects of line periodicity have been treated both analytically, with approximate linearized methods, and exactly, with nonlinear circuit simulation. Line periodicity was identified as the dominant limitation to compressed pulse risetime; with element values and spacings feasible in GaAs IC's, risetimes of 3 ps are feasible. Skin impedance of the connecting wires was also investigated; with approximate methods it was determined that skin impedance does not significantly degrade compressor performance.

A 20:1 scale model using discrete 1 pF silicon varactor diodes bonded to a coplanar transmission line on a GaAs substrate has been designed and is presently under fabrication. The scale model, which will be completed by October 1986, will compress 2 volt, 200 ps risetime, step functions to 50 ps risetime.

Two full monolithic versions of the compressor are under design. The first design, initiated in cooperation with the Microwave Systems Division of Hewlett-Packard (Santa Rosa), will generate electrical risetimes of c.a. 4 ps. The design has progressed through mask design; masks will be fabricated by 9/15/86, and circuits by 11/86.

A second, later design pursued in conjunction with Lawrence Livermore National Laboratory, which addresses risetime limitations arising from the physical layout of the structure, is under development. Masks are currently being laid out, and working devices will be fabricated by December 1986. It is anticipated that this design will generate compressed risetimes of 2-3 picoseconds.

Tapered Microstrip Couplers

Development of ultrafast electronics for frequencies up to 100 GHz and above will require unconventional circuit designs. We have developed theoretically and experimentally a novel IC 100 % coupler structure with application to very broadband millimeter- and submillimeter-wave chip-to-chip interconnects. In this application one side of the coupler is on the first chip and the other on the second chip. These couplers will provide the ultra-wideband baluns needed from microstrip to the planar lines (coplanar waveguide and coplanar strips) more suitable for ultrafast circuits. This development also provide basic designs for 3 dB hybrids and power splitters in millimeter and submillimeter systems.

Conventional microstrip couplers exhibit limited performance, specifically, in bandwidth, directivity, and low coupling values. Our work centers around the development of a warped, normal mode microstrip coupler for microwave and millimeter wave applications up to 100 GHz. In theory, this tapered structure has only a low frequency limit and its performance improves as frequency increases.

In parallel, a novel overlay technique is being developed which artificially increases the gap capacitance of coupled microstrip lines. This technique will allow the design and fabrication of conventional parallel-coupled microstrip lines with coupling values of 3 dB and higher.

Our development of a 100% tapered microstrip coupler is based on work done in 1955

by J. S. Cook, A. G. Fox, and W. H. Louisell who presented design rules and results of tapered waveguide couplers [1-3]. We began our project by theoretically verifying that propagation of coupled modes would result on tapered coupled microstrip lines. We then established design rules and boundary conditions for design and layout of this tapered microstrip structure. The resulting circuit was modeled and simulated using Touchstone, a microwave CAD program.

We have built and evaluated several scale models in order to verify the broadband nature of this device. We developed the following process steps to simplify fabrication of high resolution scale models and incur minimal costs: One, a 1:1 mask is made using a CAD graphics package to generated the pattern and a graphics plotter to cut the pattern on rubylith; Two, a substrate is cut from a piece of .250 in. Stycast and metallized by adhering a sheet of 3 mil thick copper foil; Three, the pattern is etched using standard photoresist techniques. A resolution of ± 1 mil is achievable.

We are presently working on the design and fabrication of a practical circuit which will be built on Duroid with an $\epsilon_r = 2.5$ and a thickness of 31 mils. We hope to soon be able to extend the design to a circuit which will be fabricated on a GaAs wafer for use at millimeter wave frequencies.

One of the applications of this integrated circuit structure is a very broadband 100% coupler which can be used as millimeter and submillimeter chip-to-chip interconnects. In this application one of the coupled lines is on the first chip and the other line on the second chip. Other passive component applications for the 50 to 100 GHz range include 3dB hybrids, power splitters and ultra-wideband baluns.

Electrooptic Field Modeling

One technique that has emerged in recent years as a key to understanding the operation of picosecond devices and circuits is the electrooptic sampling system [4]. Despite its increasing use, however, little has been done since the early work of Kolner [5] to describe the interactions of the electrooptic probe beam with the microwave fields of interest. In particular, little has been said of the effects of a focused Gaussian beam probing complex conductor configurations, with variable reflectivities at the front surface and with a finite interaction length dictated by the substrate thickness. To include these varied spatial alterations in the probe interaction, an analysis based on S-parameter theory has been developed. The analysis is a general approach not limited to a specific probe system. Thus other circuit and device probes, such as the charge sensing technique used in silicon devices and the Scanning Tunneling Microscope as applied to circuit measurements could also be quantitatively characterized with this approach. Below, we describe its essential features and its application to the electrooptic probing system.

Since the electrooptic interaction within a substrate is described by a perturbation of the dielectric tensor ϵ, the change in the optical signal passing through that substrate can be expressed as an optical S-parameter variation [6, 7]:

$$\Delta S_{21} = \frac{i\omega}{4} \int_{GaAs} \vec{E}^o \cdot \Delta\epsilon(\vec{E}^m) \cdot \vec{E}^o dV \qquad (1)$$

where $\vec{E}^o$ is the optical field and $\Delta\epsilon(\vec{E}^m)$ is the perturbation caused by the circuit field through the electro-optic effect. For the orientation of GaAs typically used in integrated circuits, this expression yields two terms that involve both the applied fields and the square of the optical field components. Note that both the optical fields and the applied microwave signals may be spatially varying. This integral is then performed over the volume of the GaAs, the only region where the factor $\Delta\epsilon$ is non-zero.

To simplify the evaluation of this integral for general conductor geometries, we have expressed the signal fields within the GaAs as a sum over frequency components [8]

$$E_x^m(x,z) = \sum_n A_n e^{-\alpha_n z} \cos[\alpha_n(x+\delta)] \tag{2}$$

Here α_n is a spatial wave number of order n, A_n is the relative magnitude of that spatial wave, and δ is a transverse translation factor indicating the position of the beam relative to the conductor configuration. Inserting this form of the microwave fields into (1) yields a sum of n-dependent integrals with weighting A_n.

To find the magnitude of the spatial components for specific conductor configurations, we have employed a general finite difference calculation on a IBM 3081 mainframe. A grounded back plane may be included, as well as a non-infinite ϵ_{GaAs}. These calculations yield the potential on the surface of the GaAs substrate, which is then Fourier transformed to give the factors A_n. Such FFT's have been found for several configurations to date and many more will be performed in the next month.

Once the coefficients A_n are known, the resulting ΔS_{21} may be calculated by summing the integral over the various n. A particular model must be assumed for the optical fields that includes the essential features of the focused Gaussian beam. We have examined several models, including rectangular and cylindrical abrupt cones and cylinders and combinations of these. By including a full Gaussian expression, a result may be obtained which may be expressed in closed form involving one-dimensional exponential integrals of complex argument. In most cases, these must be evaluated numerically. This may be done simply and efficiently by using the NAG routines on a DEC-20 machine. Such a calculation yields a *spatial filter function* for the A_n factors, which determines the accuracy of a measurement with the electrooptic probe.

Using this calculation, several unique properties of the electrooptic probe have been observed: spatial averaging due to finite beam size; distortion of the potential profile due to finite substrate thickness; and "crosstalk" between adjacent conductors. The first effect, the averaging of the potential on the surface, is a property of any finite width probe beam. In this calculation, however, the effect of the converging beam is also incorporated into this averaging. From this an "effective" beam width could be specified for probe users.

The distortion of the surface potential profile is a second effect of probing from the backside, unanticipated before this modeling. It is caused by the varying rate of decay of the various surface potential harmonics and the finite thickness of the electro-optic medium. Lower spatial harmonics decay much more slowly and can have significant tails beyond the substrate backside. The reduced weighting of these lower harmonics produces artificial "humps" in the measured electrooptic signal as the beam is scanned across a given conductor configuration. When combined with the variable reflectivity on the surface, such

effects may yield even larger distortions in the measurement. Further calculations are now under way to simulate measurements made on special test structures (see below).

Lastly, the alteration of the measured signal by other nearby conductors can be calculated. For probe geometries used for many GaAs SSI IC's, our calculations show that this "crosstalk" is small. However, if the conductors are very closely spaced, or if the beam if focused to a submicron spot size, such effects may become significant. Further calculations will provide guidelines for the reliability of electrooptic probe measurements as a function of spot size and conductor spacing.

To examine some of the effects described above, we designed a test structure and had it fabricated at Lawrence Livermore National Lab. The structure includes variably spaced adjacent conductors and ground planes fabricated in several different ways. A vertical assembly using standard probe arms also has been made to permit the testing of the various structures as well as the interchange of the different chips. Preliminary results from this work indicates the presence of artifacts that will be compared with the theory. These effects can be very significant and need to be understood in order for electrooptic sampling to be a reliable and accurate method of characterizing ultrafast GaAs circuits and devices.

The test structures described above also include various sizes of gaps on semi-insulating material. Although 1.06 μm radiation is below the GaAs bandgap, deep level and two-photon absorption can generate free carriers near the beam focus. The different gaps on this chip will permit the examination of such effects and others that may be taking place. Similarly, the examination of isolated MESFET's on a test chip from Tri-Quint Semiconductor will permit a more accurate description of the perturbation of integrated circuits by the intense infrared laser pulses. Modeling of these effects also may be needed to better understand the different processes involved.

In summary, we have developed an approach to modeling the electrooptic probing of GaAs integrated circuits which permits the quantitative assessment of potential inaccuracies in the measurement system. In particular, our results to date have demonstrated the presence of several forms of measurement distortion arising from the non-ideal form of the probing system. The relative importance of these is a function of conductor spacing, substrate thickness, and focusing angle. The technique is also applicable to other probing systems, and will permit a similar quantitative characterization for them.

A-1

REFERENCES

1. J.S. Cook, BSTJ **33**, pp. 807-822, Jul 1955.

2. A.G. Fox, BSTJ **33**, pp. 823-852, Jul 1955.

3. W.H. Louisell, BSTJ **33**, pp. 853-870, Jul 1955.

4. See the two recent review articles in this field: B.H. Kolner and D.M. Bloom, IEEE J. Quantum Elect., **QE-22**, 79 (1986); J.A. Valdmanis and G.A. Mourou, IEEE J. Quantum Elect., **QE-22**, 69 (1986) and references therein.

5. B.H. Kolner, PhD Dissertation, Stanford University (unpublished).

6. G.D. Monteith, "Application of the Electromagnetic Reciprocity Principle," Pergamon Press, Oxford, Ch. 5 (1973).

7. B. Lax and K.J. Button, "Microwave Ferrites and Ferrimagnetics." McGraw-Hill, New York, pp. 537-539 (1962).

8. Helge Engan, IEEE Trans. on Elect. Dev., **ED-16**, pp. 1014-1017, Dec. 1969.

PATENT DISCLOSURES

1. B.A. Auld, "Broadband Interchip Noncontact Interconnects," Feb. 28, 1986.
2. B.A. Auld, "Coupling Electrode Structure for Microstrip 3 dB Hybrids." Feb. 28, 1986.

END

11-86

DTIC